

The carbon abatement potential of high penetration intermittent renewables†

Elaine K. Hart* and Mark Z. Jacobson

Received 18th December 2011, Accepted 23rd February 2012

DOI: 10.1039/c2ee03490e

The carbon abatement potentials of wind turbines, photovoltaics, and concentrating solar power plants were investigated using dispatch simulations over California with 2005–06 meteorological and load data. A parameterization of the simulation results is presented that provides approximations of both low-penetration carbon abatement rates and maximum carbon abatement potentials based on the temporal characteristics of the resource and the load. The results suggest that shallow carbon emissions reductions (up to 20% of the base case) can be achieved most efficiently with geothermal power and demand reductions *via* energy efficiency or conservation. Deep emissions reductions (up to 89% for this closed system), however, may require the build-out of very large fleets of intermittent renewables and improved power system flexibility, communications, and controls. At very high penetrations, combining wind and solar power improved renewable portfolio performance over individual build-out scenarios by reducing curtailment, suggesting that further reductions may be met by importing uncorrelated out-of-state renewable power. The results also suggest that 90–100% carbon emission reductions will rely on the development of demand response and energy storage facilities with power capacities of at least 65% of peak demand and energy capacities large enough to accommodate seasonal energy storage.

1 Introduction

In response to a growing concern over global warming, the last decade has seen a surge in proposals for reducing the carbon dioxide emissions associated with electric power generation, many of which include large build-outs of renewable technologies including wind, photovoltaics (PVs), concentrating solar power (CSP), geothermal, wave, and tidal power. This paper

seeks to determine how the temporal characteristics of electric power demand, the variability of renewable resources, and the controls employed by renewable technologies influence the potential for a renewable portfolio to displace carbon-based generation and to reduce carbon dioxide emissions at very high penetrations. Furthermore, we seek to understand which of these factors has the strongest influence on the carbon abatement potential of a given technology, and in the case that a limit to the carbon abatement potential of intermittent renewables exists, what technologies are needed to achieve complete decarbonization of the electricity grid.

In the past, economic analyses of the carbon abatement potential of renewables have tended to assume that renewable

Department of Civil and Environmental Engineering, Stanford University, Stanford, CA, 94305. E-mail: ehart@stanford.edu; Fax: +1 650 7237058; Tel: +1 650 7212650

† Electronic supplementary information (ESI) available. See DOI: 10.1039/c2ee03490e

Broader context

The reliable integration of renewable resources on to the electricity grid represents an important step toward decarbonizing the electric power sector and mitigating global climate change. This step is complicated by both the variability and the uncertainty associated with power output from renewable resources, like wind and solar power. Analyses that seek to quantify system reliability, reserve requirements, and the carbon dioxide emissions associated with operating these reserves have historically relied on simulations with high temporal resolution (typically an hour or less) and with stochastic treatments, both of which increase the computational complexity significantly. However, energy-economic models capable of analyzing the costs and economic impacts of different decarbonization strategies or policies typically use time scales of one year and cannot accurately resolve the phenomena associated with intermittent renewables. In this paper, we develop a parameterization of the results from higher temporal resolution simulations that can be implemented in large-scale energy-economic models. This effort contributes to the improved economic treatment of renewable power sources in analyses used by policymakers and may provide additional insight regarding technological cost targets for innovators.

energy contributes no operational carbon emissions and that the carbon abatement potential of a renewable technology can be approximated from the carbon intensity of the displaced fossil generation.¹ This assumption, while qualitatively intuitive, neglects some potentially important effects on the system-wide carbon emissions. These effects include the emissions associated with the construction and decommissioning of the renewable facilities and the added emissions associated with the operation of fossil fuel-based plants to reliably meet demand in the context of a more variable and less predictable generation fleet. The construction/decommissioning effects have been largely dealt with in life-cycle analyses of wind and solar.^{2–6} Here we focus specifically on the carbon emissions associated with intermittency mitigation.

The effects of intermittent renewable power on the operation of conventional dispatchable generation has been investigated predominantly using dispatch models. Broadly speaking, conventional dispatchable generators must operate at lower capacity factors to balance renewable generation and to provide adequate reserves to maintain reliability than in current systems. Reduced capacity factors also reduce the efficiency of the plant, increasing fuel consumption, carbon dioxide emissions, and cost per unit of energy generated. Studies focusing on the associated costs of these inefficiencies^{7–10} have found that the cost of grid integration depends on the resource, the system into which it is being integrated, and most important in the context of this study, the energy penetration of the renewable technology. The effects of these inefficiencies on carbon dioxide emissions have been modeled for several systems, including the Irish system with wind power capacities up to about 11% of total capacity;¹¹ a portfolio of wind farms across the Midwestern US;¹² the California ISO load with renewable energy penetrations up to 80%;¹³ and systems in which natural gas is used to supplement wind power to provide baseload power.¹⁴ These analyses have found that wind power reduces the total system-wide carbon dioxide emissions compared with the current system, though the reductions are less than would be expected from the simple generation displacement assumption.

If the grid integration cost analyses are any indication of what to expect in carbon abatement analyses, one might expect that the carbon abatement potential of renewables is a function of the technology's penetration. In this study, we therefore seek to describe the carbon abatement potentials of different renewable generation technologies and renewable portfolios across a wide range of energy penetrations. We first introduce a parametric description of the carbon abatement potential of renewables as a function of installed capacity. We then apply this method to specific technologies of interest, including wind, centralized CSP, rooftop PVs, and baseload geothermal, in a case study of the California ISO operating area. We also demonstrate how this method can be used to compare portfolios of renewable technologies and we discuss sensitivities to the growth (or decline) of system-wide electric load. Finally, we use simulation results to provide insights into the capabilities required of new technologies in order to achieve a fully decarbonized electric power sector.

2 Theory

The carbon abatement potential of a renewable generating technology has been defined broadly as the carbon emissions

avoided by a unit increase in the penetration of the technology. The carbon abatement potential depends strongly on both the behavior of the renewable technology and the composition of the conventional generation fleet. It may also depend on the penetration of the renewable technology, as the operating procedures of conventional plants are adjusted to mitigate intermittency. Here we describe a quantitative approach to describing this dependence on penetration for different types of renewable technologies.

In this analysis, the carbon intensity of a given electricity system is reported as the metric tonnes of CO₂ emitted per MWh of total generated energy. For a renewable technology, this system-wide carbon intensity can be described as a function of the installed capacity of the renewable technology (in GW), the annual energy that it generates (in GWh), or its energy penetration (in % of total delivered energy). Previous modeling studies have suggested that the system-wide carbon intensity drops linearly with the energy generation (or energy penetration) associated with wind and solar power,^{13,14} a conclusion that is supported by the simulations presented in this analysis. The carbon intensity, E , can therefore be approximated by the following equation:

$$E_{\alpha}(\alpha) = E_0 - \chi\alpha \quad (1)$$

where E_0 is the carbon intensity at zero penetration, α is the energy penetration the technology, and χ we refer to as the carbon abatement rate of the technology.

While this equation is simple, the cost of developing renewable power depends on the installed capacity, rather than the energy penetration. Economic analyses or long-term planning analyses may therefore relate carbon abatement to cost by expressing the carbon intensity as a function of installed capacity. This function can be approximated first by determining the energy penetration of the technology in the system of interest as a function of its installed capacity, and then substituting this function into eqn (1).

In this analysis, the energy penetration is approximated first by expressing the annual energy generated by the technology as a function of the installed capacity, $G(C)$, then dividing by the total annual energy generated in the entire system, G_{tot} . The generation function depends on the nature of the resource, the energy conversion technology and its associated controls, and the composition of the rest of the electric power system. For small penetrations, this function is typically linear, with a slope proportional to the expected capacity factor of the technology. We refer to this behavior as the “linear regime.” At larger penetrations, in the “curtailment regime,” the generation function may exhibit sublinear behavior due to curtailment in hours when the generation would otherwise exceed demand.¹⁵ We will show in this analysis that the generation function can be approximated by eqn (2).

$$G(C) = \begin{cases} kC & \text{if } C < C_q \\ G_{\infty}(1 - e^{-\gamma C}) & \text{if } C \geq C_q \end{cases} \quad (2)$$

where k is the expected capacity factor times 8760 h; C_q is the minimum capacity at which curtailment of generation gives rise to a sublinear generation function; G_{∞} is the theoretical maximum energy generation that can be integrated into the

system from the technology of interest, neglecting land and water use constraints; and γ describes the rate at which the annual generation approaches G_∞ in the curtailment regime. It follows that the maximum theoretical energy penetration of a technology, α_∞ , is:

$$\alpha_\infty = \frac{G_\infty}{G_{tot}} \quad (3)$$

The present study assumes that excess generation in the curtailment regime is not utilized. More efficient systems could potentially utilize this electricity for other energy services, like heating, transportation, or industrial processes *via* electrification or hydrogen/fuel production, leading to additional carbon emissions reductions in other sectors. As is discussed in Section 4.4, this energy could also be used with energy storage systems to displace conventional generation. While these technologies are not directly treated in this analysis, our results motivate continued research and development of energy storage systems and the electrification of additional energy services.

When eqn (1) holds, the carbon intensity of the system can be described by the following function of the installed capacity of the technology or portfolio:

$$E_C(C) = \begin{cases} E_0 - \chi kC/G_{tot} & \text{if } C < C_q \\ E_0 - \chi\alpha_\infty(1 - e^{-\gamma C}) & \text{if } C \geq C_q \end{cases} \quad (4)$$

This function is referred to as the “carbon curve” for the remainder of this paper. One potential use of this curve is to back out the maximum theoretical carbon abatement potential of a renewable technology, $\chi\alpha_\infty$, and the minimum theoretical carbon emissions from the buildout of the technology, $E_0 - \chi\alpha_\infty$.

Fitting aggregated energy generation and carbon emissions results from dispatch simulations to the generation function in eqn (2) and the carbon curve in eqn (4) provides a number of fit parameters that provide insight into the effectiveness of renewable technologies for displacing conventional generation and reducing carbon dioxide emissions. These metrics are described in Table 1. It is important to note that most of these parameters will depend on both the nature of the resource and the nature of the electric power system under study. The present study includes an application of this analytical approach to a specific power system with its associated wind and solar resources. While the precise metrics identified for this system are not universal, the insights provided by these metrics may aid utilities,

policymakers, and engineers in identifying new decarbonization strategies.

3 Methodology

Generation functions and carbon curves were produced for each technology and portfolio of technologies using a Monte Carlo least-cost dispatch model for the operation of electric power systems with large penetrations of intermittent renewables¹³ (See the ESI† for a description of the model updates that were undertaken in preparation for this analysis). The model includes approximate historical generation from existing hydroelectric plants, generation from baseload geothermal plants, and modeled power output from wind and solar facilities based on site-specific installed capacities, input meteorological data, and statistical models for resource availability.

The following controls are available to each technology: wind power is allowed to curtail in real-time; CSP curtailment is scheduled on a day-ahead basis; rooftop PVs have no curtailment controls and operate as must-run capacity in real-time, except in the analysis presented in Section 4.2; baseload plants (geothermal or nuclear) operate at full capacity in all time steps, except in the case of forced outages; hydroelectric plants are scheduled on a day-ahead basis and operate as must-run capacity in real-time; and natural gas plants (equipped with highly flexible Siemens-Westinghouse 501FD turbines) are scheduled on a day-ahead basis, but are allowed to ramp up to the scheduled maximum capacity and down to zero power in real-time. Baseload, hydroelectric, and solar power facilities therefore reduce the downward flexibility of each generation portfolio unless additional controls are incorporated.

The model approximates the necessary capacity and dispatch of natural gas plants necessary to ensure that the system meets a loss of load expectation of 1 day in 10 years. It also approximates the carbon dioxide emissions associated with operating the natural gas plants. The model was run using hourly meteorological and load data for the California ISO operating area over the years 2005 and 2006. Generation functions and carbon curves were produced by running the dispatch simulation over a range of different input installed capacities. The zero-renewables base case referred to throughout this analysis assumes that all load is met from natural gas and existing hydropower plants. This portfolio was found to have a carbon intensity of 0.29tCO₂/MWh.

Table 1 Summary of the carbon abatement and grid integration metrics that are used to compare the carbon abatement potentials of intermittent renewables. Note that in the unit tCO₂/MWh, the MWh refers to the annual system load, not the annual generation from the renewable portfolio

	Symbol/Equation	Description
Carbon Abatement Metric		
Carbon Abatement Rate	χ	tCO ₂ /MWh avoided per % of renewable penetration
Maximum Carbon Abatement	$\chi\alpha_\infty$	The maximum theoretical reduction in carbon intensity achievable with the technology or portfolio, tCO ₂ /MWh
Grid Integration Metric		
Low-Penetration Capacity Factor	$k/8760$ h	Average generation, as a fraction of the installed capacity for low penetrations
Maximum Energy Penetration	α_∞	The limit of the generation function as the capacity approaches infinity, divided by G_{tot}
Curtailment Point	C_q	The minimum capacity (GW) at which generation from the technology must be curtailed to exactly meet demand

The metrics in Table 1 were determined for each generation function and carbon curve using least-squares fits to the simulation results. Since the curtailment point is initially unknown, every possible demarcation between linear and curtailment regime data was considered and the best fit to eqn (2) across all scenarios was chosen.[‡] The curtailment point was then found by solving the following equation for C_q :

$$kC_q = G_\infty(1 - e^{-\gamma C_q}) \quad (5)$$

For most analyses, the carbon curve was constructed from the generation function by determining χ from a least-squares linear fit of the carbon intensity to the energy penetration. For some portfolios, however, the linear assumption (eqn (1)) breaks down at very high penetrations so that the constructed carbon curve overestimates the maximum theoretical carbon abatement of the portfolio. For these portfolios, a separate fit is employed to determine the maximum theoretical carbon abatement, E_∞ , and the minimum theoretical carbon intensity, $E_0 - E_\infty$:

$$E_C(C) = \begin{cases} E_0 - \chi kC/G_{tot} & \text{if } C < C_q \\ E_0 - E_\infty(1 - e^{-\lambda C}) & \text{if } C \geq C_q \end{cases} \quad (6)$$

In the first set of simulations, each renewable technology (wind, PVs, CSP, and geothermal) is investigated on its own in order to directly compare the carbon abatement potentials of technologies that exploit different types of resources and have different control schemes. The next set of simulations explores portfolios that combine wind and solar power in different ratios to determine the extent to which synergies between the resources improves the high penetration carbon abatement potential. From these simulations, a single portfolio of wind and solar power is selected for use in another set of simulations that explore the effects of building must-run baseload power (geothermal or nuclear) on the carbon abatement potential of intermittent renewables. Finally, an analysis is performed that tests the sensitivity of the fitting parameters to modification of the input load, which is intended to simulate either efficiency improvements or growth of electric power demand over time.

4 Results and discussion

4.1 Single renewable technology simulations

The results from a set of dispatch simulations with different capacities of wind, centralized CSP, rooftop PVs, and geothermal plants are shown in Fig. 1(a) and 1 (b). Fig. 1 (a) shows the generation functions (with the corresponding fits to eqn (2)) and Fig. 1 (b) shows the carbon curves. The parameters for the fit functions shown in each figure are listed in Table 2. The fit parameters illustrate the limits of the generation functions and carbon curves as the installed capacities approach infinity. In addition to these “theoretical” metrics, which are useful for approximating each function, Table 2 also includes a set of “developable” maximum energy penetrations and minimum carbon intensities to reflect the limitations imposed by the

[‡] It should be noted that the curtailment points can be higher than the peak demand for portfolios containing PVs because PV capacities are stated before inverter, dirt, and mismatch losses, so that the peak power output is less than the installed capacity.

developable land (or rooftop) area available to each technology. For most technologies, the theoretical limits far surpass the developable limits, with the exception of CSP, which appears to be limited predominantly by grid integration issues, rather than land availability.

The generation functions and carbon curves illustrate some of system-level effects of the resource availability and control schemes associated with each renewable technology. The low-penetration capacity factors reflect the average availability of the resource. Baseload geothermal plants have by far the steepest generation curves in this regime. However, the maximum buildout of geothermal is limited by hours in the simulation when the load minus the other must-run generation is small. The high capacity factors of baseload systems therefore lead to rapid carbon dioxide emissions reductions at low penetrations, but the limited flexibility of these systems leads to a maximum theoretical carbon abatement potential of only 41% (20% if limited to the developable resource). The theoretical limitation would hold for any low- or zero-emitting baseload technology, including nuclear power.

Buildout of PVs is similarly limited by the hours when the the load minus the other must-run generation is small and must-run PV output is large. PVs have the advantage of generating during the day, when the load is higher, but the low capacity factor of PVs translates into a low maximum energy penetration (19%, or 15% if limited to rooftops) and low maximum carbon abatement

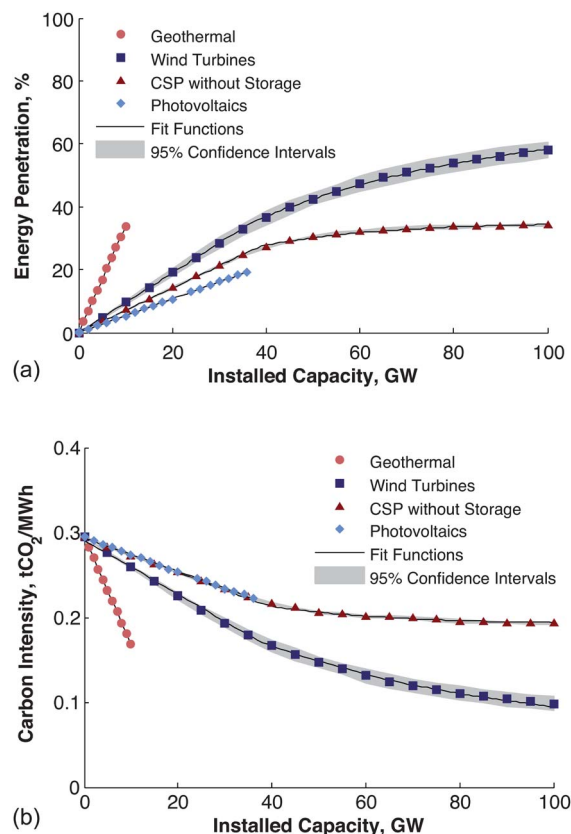


Fig. 1 (a) Generation curves; and (b) Carbon curves for single technology buildout scenarios in the California ISO with load and resource data from 2005–06. The 95% confidence intervals are based on the standard deviations of the results from the Monte Carlo simulations, which exceed the 95% confidence intervals of the fit functions.

Table 2 Calculated values of the carbon abatement and grid integration metrics for each technology, assessed for integration into the 2005–2006 California ISO operating area with conventional hydroelectric and natural gas plants. Below the theoretical metric based on fits to the generation and carbon curves are the practical limitations of each technology based on land exclusion and available rooftop area analyses.^{16–19} For context, each land/rooftop area constraint is accompanied by the corresponding fraction of California's total land area in brackets. The resource-limited maximum penetration and minimum carbon intensity are calculated from the resource-limited capacity and the fit functions for the generation and carbon curves. Note that in the unit tCO₂/MWh, the MWh refers to the annual system load, not the annual generation from the renewable portfolio, so that the carbon abatement rate refers to reductions in the entire system's carbon intensity

	Wind	Centralized CSP	Rooftop PVs	Geothermal
Low-Penetration Capacity Factor (%)	27.8 ± 0.3	20.8 ± 0.2	15.68 ± 0.02	99.350 ± 0.001
Curtailement Point (GW)	37 ± 5	38.7	36 ± 1	10 ± 1
Maximum Theoretical Energy Penetration (%)	67.8 ± 0.9	35.1 ± 0.4	19 ± 1	34 ± 3
CO ₂ Abatement Rate (tCO ₂ /GWh per %)	3.36 ± 0.4	2.91 ± 0.5	3.71 ± 0.5	3.73 ± 0.03
Minimum Theoretical CO ₂ Intensity (tCO ₂ /MWh)	0.063 ± 0.008	0.192 ± 0.004	0.222 ± 0.006	0.17 ± 0.01
Land/Rooftop Area Constraint (km ²)	9,800 [2.5%]	1,600 [0.4%]	260 [0.07%]	—
Maximum Developable Capacity (GW)	73.6 ²⁰	76.2 ^{16,17}	28.2 ¹⁸	4.8 ¹⁹
Maximum Developable Energy Penetration (%)	51.9	33.3	15.1	16.2
Minimum Developable CO ₂ Intensity (tCO ₂ /MWh)	0.12	0.20	0.24	0.23

potential (23%, or 17% if limited to rooftops). As is discussed in Section 4.2, inclusion of curtailment controls dramatically improves the maximum carbon abatement potential of PVs to 56% (including both rooftop and centralized systems).

For this set of simulations, both the wind and CSP plants are allowed to curtail their power output in hours when the generation would otherwise exceed demand. This allows for the buildout of wind and CSP to exceed the curtailment point, resulting in high maximum developable energy penetrations (52% and 33%, respectively). Wind power outperforms CSP at low penetrations due to its larger capacity factor and at high penetrations because CSP cannot generate at night (without thermal storage) regardless of its capacity. Furthermore, the maximum developable carbon abatement potential of wind power (58%) exceeds that of baseload geothermal, but must do so through extensive overbuilding and curtailment.

These results demonstrate the advantages of improved flexibility in the operation of renewable energy systems, in the absence of controllable loads and large-scale energy storage deployment. Geothermal systems that are able to ramp up and down as well as PVs with inverters that are equipped with curtailment controls and communications can contribute to larger renewable energy penetrations. Despite reductions in overall capacity factor, curtailment allows for increased maximum capacities and hence increased maximum carbon abatement potential. However, dramatically reduced capacity factors make renewable projects in the context of very high penetrations even less financially viable in the absence of incentives or new markets.

4.2 Portfolios of intermittent renewables

Studies have shown that combining different renewable technologies into single portfolios may improve the portfolio's performance due to increased diversity.^{21–24} In order to test this hypothesis in the context of carbon abatement, the model was run with different portfolios of renewables. First, a set of simulations explored the potential synergies between wind and solar power by repeating the build-out scenarios of the single-technology studies, but with constant fractions of each portfolio devoted to wind and to solar technologies.

For these simulations, we assumed that all solar sites are developed with PV systems that include curtailment controls and communications with system operators or aggregators. This significantly reduces the sizes of the scheduling and dispatch problems from the case where both PVs and CSP plants are modeled separately, while also allowing for the exploration of very high solar power penetration scenarios. The metrics described in Table 1 were calculated for each type of portfolio and are shown as functions of the portfolio composition in Fig. 2(a)–(e). It is important to note that at very high penetrations, the linear assumption in eqn (1) breaks down, so that eqn (4) overestimates the minimum developable carbon intensity. For these simulations, eqn (6) was instead used in order to determine the minimum theoretical carbon intensity. The assumption that PVs, rather than CSP plants are constructed at the large centralized solar sites across the state also changes the maximum developable capacity of solar from 104.4 GW to 202 GW (assuming a power density of 10W-installed/sq. ft¹⁸).

As shown in Fig. 2(a), the low-penetration capacity factor deviates very little from the weighted average of the individual wind and solar capacity factors, so the benefits of combining wind and solar at low penetrations are not apparent. Similarly, the carbon abatement rate is not significantly affected by the composition of the renewable portfolio (Fig. 2(b)). At high penetrations, the advantages of combining wind and solar are more apparent. Fig. 2(c)–(e) show that combining wind and solar into a single renewable portfolio (with curtailment controls and the appropriate communications) yields larger curtailment points and maximum energy penetrations, as well as lower minimum carbon intensities, when compared with the single-technology performance. These results suggest that at low penetrations, it is most effective to build out the higher-capacity factor technology (wind power), but at very high penetrations there is a significant advantage in combining resources to achieve higher energy penetrations and lower carbon emissions *via* reduced curtailment.

Additional simulations were undertaken in which baseload geothermal (or nuclear) is integrated with a portfolio of wind and solar. The wind/solar composition is fixed at 30%-wind/70%-solar (by capacity) for these simulations to take advantage of the

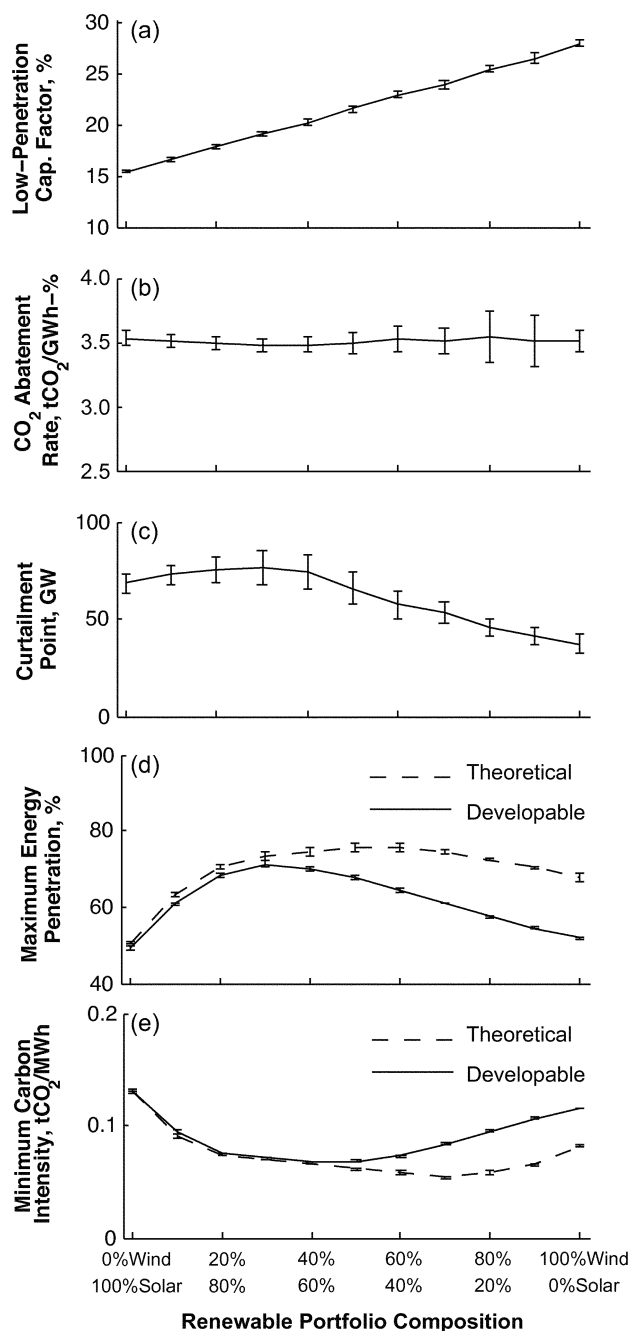


Fig. 2 Generation and carbon curve fitting parameters for renewable portfolios consisting of different compositions of wind and solar power. These simulations assume that all solar power is provided by curtailable PV systems. The fit parameters include: (a) Low-penetration capacity factor; (b) Carbon abatement rate; (c) Curtailment point; (d) Maximum theoretical energy penetration of the renewable portfolio and maximum developable energy penetration based on land area constraints; and (e) Minimum theoretical carbon intensity of the system and minimum developable carbon intensity based on land area constraints.

improved performance at high penetrations illustrated in Fig. 2(d) and 2(e). The introduction of geothermal power both increases the renewable energy penetration and reduces the carbon intensity of the system for build-outs up to 9GW. Above 9GW, the dispatch problem becomes infeasible in hours of low

load and high must-run capacity. The contributions of baseload power to both the maximum energy penetration and maximum carbon abatement potential of a portfolio consisting of wind, solar, and geothermal power are shown in Fig. 3(a) and 3(b). As the capacity of baseload power increases, the benefits of baseload power are largely offset by reduced performance of the wind and solar portfolio at high penetrations. This trade-off is due to the additional wind and solar curtailment that accompanies an increase in must-run capacity on the system. Renewable portfolios with baseload power therefore see only slight increases in the maximum renewable energy penetration and maximum carbon abatement potential over those containing only wind and solar.

The conclusions that can be drawn regarding baseload power depend on the type of energy resource being exploited. If baseload power can be provided from non-emitting renewable resources (e.g. binary geothermal power plants), then it is well suited for achieving rapid carbon emissions reductions in early mitigation stages. In these simulations, baseload power was capable of displacing up to 40% of the system's carbon dioxide emissions with capacities up to 9GW. Beyond 9GW, however, further reductions in carbon dioxide emissions must come from significantly less efficient, but more flexible systems, like curtailable wind and solar plants. If baseload power is instead produced from a non-renewable resource, like nuclear power, then the same carbon dioxide emissions reductions are possible, but the maximum renewable energy penetration (from wind and solar power) drops from 71% with no nuclear power to 46% with 9GW of nuclear power.

4.3 Sensitivity to electricity demand

The results of this analysis are highly dependent on both the nature of the renewable resources and the nature of the electricity demand. While the characteristics of the wind and solar resources will remain largely constant over long periods of time (on the order of decades), the electric load is likely to undergo significant changes. Population growth will likely drive growth in

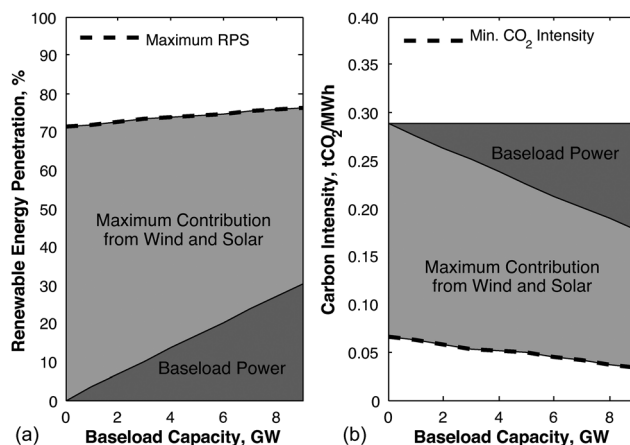


Fig. 3 The effects of baseload power on (a) the maximum renewable energy penetration, and (b) the minimum system-wide carbon intensity. The energy penetration and carbon intensity are both plotted as functions of the total installed capacity of baseload power in the system. Shaded areas represent contributions from baseload power vs. intermittent renewables (wind and solar).

the electricity demand over the next several decades, while efficiency improvements may lead to reduced demand per capita (and potentially reduced aggregate demand if efficiency improvements are aggressively adopted). In order to investigate the effects of future demand growth (or decline) on the carbon abatement potential of renewables, an additional set of simulations was undertaken for the 30%-wind/70%-solar portfolio with an adjusted load.

Using historical and projected data, the California Energy Commission estimates that between 1990 and 2018, California's peak demand will grow at an average annual rate of 1.35%, while its annual electrical energy consumption will grow at an average annual rate of 1.09%.²⁵ For simplicity, the present analysis assumes that the peak demand and electricity consumption grow (or decline) at the same rate, so that the load time series data over 2005 and 2006 can simply be multiplied by a scale factor (or "load modifier") to produce each load scenario.

The sensitivity of the maximum energy penetration of the wind/solar portfolio to changes in electricity demand is shown in Fig. 4(a). The maximum theoretical energy penetration of renewables, α_{∞} , increases with load growth, owing to increased overall system flexibility. Since the model includes existing hydroelectric power regardless of load growth or decline, the fraction of load served by must-run hydroelectric plants is reduced as the electricity demand increases over time, resulting in increased downward flexibility. This increased flexibility is reflected in the curtailment point, which scales approximately with the peak demand. Trends in the maximum developable or achievable energy penetration, α_{max} , which is limited by rooftop area and land availability, differ from the trends in α_{∞} . For low electricity demands (less than 110% of the 2005–2006 demand), intermittent renewable penetration is limited by system flexibility, while for higher electricity demands, renewable penetration is limited by land and rooftop availability. For this reason, α_{max} decreases as the load grows beyond 110% of the 2005–2006 demand. Despite this reduction in α_{max} , the total maximum energy (in MWh) produced from renewables over the simulation period (shown in Fig. 4(b)) increases as the load increases due to reduced curtailment.

The sensitivity of the system-wide carbon intensity to changes in electricity demand is shown in Fig. 5(a). The carbon intensity of the conventional portfolio increases with demand growth because additional demand growth is assumed to be met from natural gas plants (as annual generation from hydropower is held constant). Recall that the total amount of carbon dioxide emitted annually is the product of the carbon intensity and the annual generated electrical energy, so that an increasing carbon intensity with demand implies that the carbon emissions grow faster than the demand, barring the growth of the renewable portfolio (See Fig. 5(b)). As a corollary, carbon emissions are reduced more rapidly than reductions in demand due to efficiency improvements and conservation. In the system under study, a reduction in demand by 10% avoids 9.6MtCO₂, or 13% of the base case emissions.

Unfortunately, conservation or efficiency improvements have a similar effect on the maximum carbon abatement potential of intermittent renewables as the introduction of baseload power unless must-run capacity is simultaneously retired. Reduced system flexibility limits the additional gains that can be made by building out renewables so that while

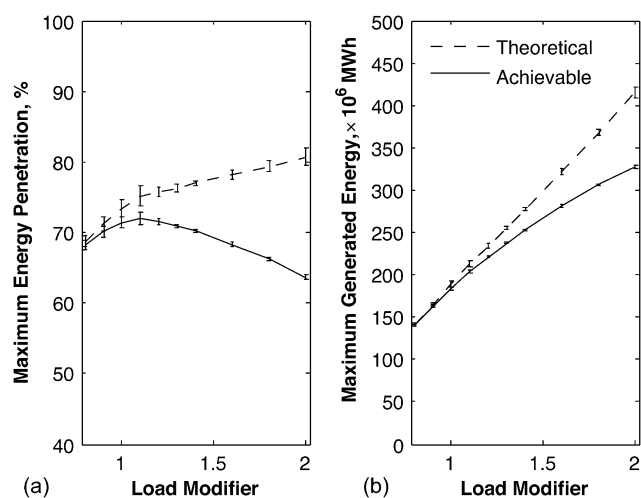


Fig. 4 The effects of increasing or decreasing electricity demand on the maximum energy penetration of intermittent renewables, in terms of (a) energy penetration as a fraction of total demand, and (b) absolute energy generated over the two-year simulation. All renewable portfolios consist of 30% wind and 70% solar, by capacity. The effects of improved efficiency are demonstrated by moving along each curve to the left and the effects of electricity demand growth are demonstrated by moving along each curve to the right.

shallow emissions reductions can be met fairly easily with demand reduction, deeper carbon emissions reductions will rely on a combination of renewables and dramatically improved system flexibility.

4.4 Insights toward complete decarbonization

This analysis has shown that despite the abundance of renewable resources in California, the maximum carbon abatement

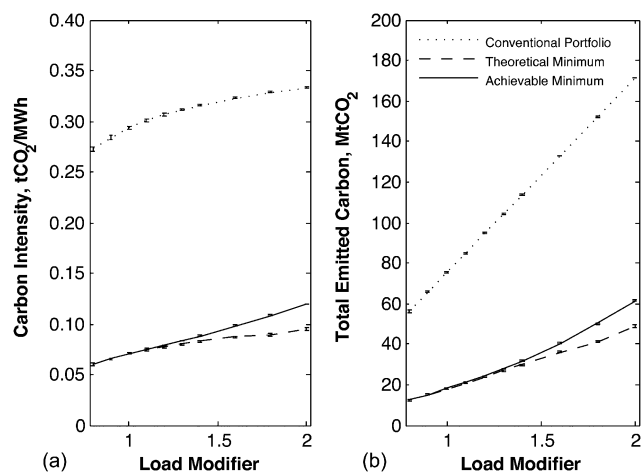


Fig. 5 The effects of increasing or decreasing electricity demand on the minimum electric power sector carbon dioxide emissions, in terms of (a) carbon intensity as a fraction of total demand, and (b) absolute carbon emissions over the two-year simulation. All renewable portfolios consist of 30% wind and 70% solar, by capacity. The effects of improved efficiency are demonstrated by moving along each curve to the left and the effects of electricity demand growth are demonstrated by moving along each curve to the right.

potential of renewable resources in the state (barring an energy storage fleet) appears to fall short of complete decarbonization over the 2005–2006 simulation period. This is due in part to hours when renewable resources are insufficient to completely meet the demand. In addition to the emissions associated with natural gas generation in these hours, some background emissions are also associated with the operation of large fleets of spinning reserves to ensure system reliability. In order to completely decarbonize the electricity sector, both of these roles will need to be served by zero-carbon technologies. The timing and magnitude of these demands for both additional balancing generation and reserves are therefore of interest to anyone seeking to comment on the appropriateness of new technologies for contributing to a zero-carbon electric power sector.

In order to investigate the balancing generation and reserve requirements in more detail, an additional simulation was performed with 30GW of wind power, 70GW of curtailable PVs, 9GW of baseload geothermal power, and existing hydropower. Fig. 6(a) and (b) show the timing and magnitude of scheduled and utilized natural gas capacity in these simulations, respectively. The data are broken down by day of the year and time of day in order to show both seasonal and daily trends. Although there is little to no utilization of the natural gas capacity throughout most of the year, there are some times when up to 25 GW of capacity are required for both load balancing and maintaining reserves. These rare events tend to occur in the late summer through autumn, when much of the hydroelectric resources have been exhausted for the year. In this simulation, the natural gas reserves are also typically used at night, when solar power is unavailable and the wind resource may be unreliable. In addition to these extreme events, a background of at least 5–10GW of natural gas are required for reserves even in hours when the renewable resources meet demand. Similar trends were found for a portfolio favoring wind power over solar, though the diurnal pattern was less substantial (See ESI†).

The natural gas utilization patterns provide some insight regarding the sizes and characteristics of alternative technologies that could contribute to complete decarbonization. The constant background reserves, for example, suggest that the system will require about 5–10GW of short-term reserves to maintain system reliability. Meeting some of this reserve requirement may be a logical role for demand response systems that can respond to real-time pricing or direct signals from the system operator to

delay energy use in hours when the system is constrained. Some of these reserves may also be served by underutilized hydropower plants, the reserves from which were not modeled in this analysis.

In addition to these short-term reserves, additional power (about 10 GW) is required on a predominantly diurnal basis for the solar-dominated portfolio. This suggests that energy storage on the order of 6–12 h may be well-suited for the further decarbonization of portfolios consisting of large build-outs of solar power. This may take the form of thermal energy storage systems at CSP plants or on- or off-site storage if the prices of PVs drop sufficiently to spur large-scale deployment. Some of this diurnal energy requirement may also be met by shifting demands from the evening to the daytime when the solar resource is adequate, a result that is unintuitive in the context of the current system. The strong seasonal component in the natural gas utilization pattern also suggests that seasonal storage facilities with very large energy capacities will be required to achieve complete decarbonization.

Exact sizing of storage systems necessary to achieve complete decarbonization is beyond the scope of this paper, but a simple storage size minimization with a portfolio of 70GW solar, 30GW wind, 9GW baseload, and existing hydropower yielded a lower bound of 20,000GWh of storage in order to meet demand, assuming perfect prior information and a storage round-trip efficiency of 40%. The power capacity of these storage systems would aggregate to approximately 65% of the peak demand. Rather than serving as a supplementary source of power, the storage systems would largely decouple real-time generation from real-time demand, constituting a much more significant paradigm shift in the electric power sector.

Two additional points must be considered with regard to complete decarbonization. First, the energy storage and demand response systems discussed in this section would significantly improve system flexibility, making room for deeper cuts from renewable baseload power and demand reductions *via* efficiency improvements and/or conservation. The conclusions reached in Sections 4.2 and 4.3 change dramatically for systems with energy storage technologies. While the details are beyond the scope of this paper, the role of baseload power and demand reduction in the context of energy storage deployment remains a rich area for future investigation. Second, the 1 h time step used in these simulations precludes an analysis of the regulation requirements on these systems, but the large portfolios of demand response and energy storage technologies that would be needed to reach

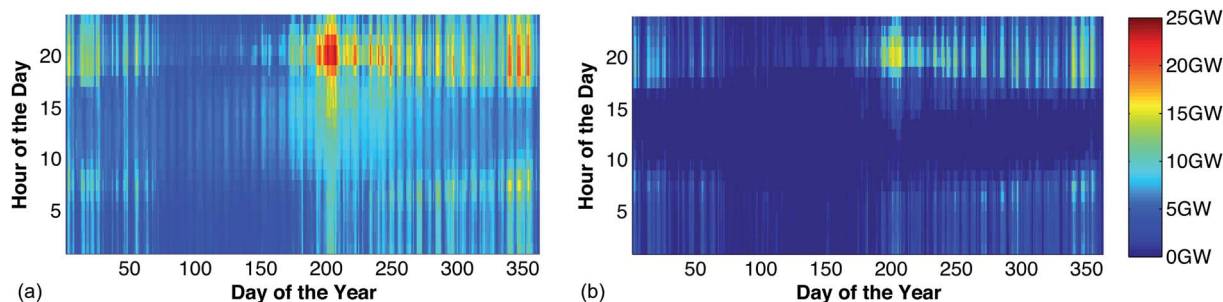


Fig. 6 The average (a) available, and (b) utilized natural gas generating capacity in each hour of the year for a simulation of the California ISO over 2005–2006 with a renewable portfolio consisting of 70GW solar, 30GW wind, and 9GW geothermal power.

complete decarbonization could likely also provide regulation services if the proper controls were implemented.

5 Conclusions

A parameterization of results from grid integration analyses was presented in order to describe the carbon abatement potentials of renewable electric generation technologies across a wide range of energy penetrations. The fit parameters were used to compare the carbon abatement potentials among different resources and control schemes, to quantify the benefits of combining renewables in different portfolios, and to examine the sensitivity of the carbon abatement potential of intermittent renewables to trends in the electricity demand.

Simulations of the build-out of single technologies reinforced the importance of improving the capacity factor of renewable resources for meeting low to moderate emissions reductions targets. Furthermore, achieving deeper carbon emissions reductions with renewables (greater than about 20% in the system under study) relies on the use of curtailment controls and communications between renewable facilities and the system operator or an aggregator. With these controls, renewables were capable of displacing a significant fraction of the system-wide emissions - about 58% for wind power and 30% for CSP. PVs were simulated with and without controls, yielding an increase in the maximum carbon abatement potential from about 20% to over 50% by including curtailment controls and communications, despite the associated capacity factor reductions at high penetrations.

Potential synergies between wind and solar power were also investigated by simulating the build-out of different compositions of renewable portfolios. It was found that at low penetrations (in the linear regime), the combined effects of wind and solar are approximately additive, but that portfolio performance is enhanced by combining wind and solar at very high penetrations. A portfolio of 30%wind/70%-solar was found to have a maximum carbon abatement potential of 79%, compared with 58% and 56% for wind and solar alone, respectively. The improved high penetration performance of combined portfolios was due to a reduction in the incidence of curtailment, suggesting some degree of complementarity between wind and solar resources. These results also suggest that portfolio performance at high penetrations may also be improved by importing uncorrelated renewable power from other states. The effects of increasing the catchment area on the carbon abatement potential of renewables remains an opportunity for further investigation.

Renewable baseload power, from binary cycle geothermal plants for example, was identified as an efficient way to achieve low to moderate reductions in carbon dioxide emissions, but the potential of baseload systems to achieve deep reductions was limited by a lack of downward controls in hours of low electricity demand. Baseload power was also found to inhibit the ability of intermittent renewables to displace additional carbon-based generation due to reduced overall system flexibility, leading to only moderate increases in the maximum carbon abatement potential of renewable portfolios that include baseload power (89%) over those that do not (79%).

Demand reduction *via* energy efficiency improvements or conservation efforts yielded similar behavior to the build out of baseload power in that it efficiently reduced both the carbon

intensity of the conventional portfolio and the minimum developable carbon intensity of a renewable portfolio. However, since the curtailment point scales approximately with the peak demand, efficiency improvements and/or conservation slightly inhibit the ability of renewables to achieve even deeper emissions reductions unless must-run capacity is simultaneously retired. Even though demand reductions and renewables do not appear to be synergistic at high penetrations, the benefits of energy efficiency and conservation should not be ignored. In the system under study, a reduction in demand by 10% avoids 9.6MtCO₂, or 13% of the base case emissions. For comparison, achieving this same level of emissions reductions from the base case would require 2.9 GW of baseload power plants or 12 GW of wind turbines.

This analysis also found that local renewables were capable of displacing the vast majority of carbon-based generation in California. A portfolio of 73.6GW of wind turbines, 172 GW of curtailable PVs, and 9GW of renewable baseload power (about double the approximate state-wide geothermal resource) was found to displace 89% of the base case carbon dioxide emissions. However, eliminating the remaining emissions associated with load balancing and spinning reserves appears to require a more significant paradigm shift in the electric power sector. While demand reduction *via* energy efficiency and conservation might reduce the installed capacities (and hence the costs) required to meet a given renewable portfolio standard, complete decarbonization seems to rely critically on improved system flexibility. Some of this flexibility could come from changes in human behavior and/or the adoption of demand response technologies, but the large power capacities required to meet current reliability standards suggest that very large scale energy storage will also be required to decouple the electricity demand from the real-time power availability of renewables.

Although this analysis focused on the state of California, some of the general results may apply to other systems as well. The ease with which a region can meet a renewable portfolio standard, in terms of built capacity and cost, will depend on the available resources and the electric load. The generation and carbon curves will therefore differ across different regions. However, the steps required to achieve complete decarbonization may be more universal. The simulations show that without storage, conventional dispatchable capacity must be available for the rare events in which renewable output is very low relative to the load. While the frequency of these events is low, the magnitude of lost load in these events would be unacceptably high. In areas that do not have ample hydroelectric capacity to handle these events, complete decarbonization will rely on measures similar to those identified for California. These measures include: further reductions in the capital costs of renewable generators; continued research into energy storage, specifically toward cost reduction and improved stochastic controls for load balancing intermittent renewables; and significant investment in upgraded transmission, distribution, and communication infrastructure to support renewable build-out and demand response technologies. These technical steps toward a decarbonized electric power sector must also be accompanied by a willingness on the part of utilities, system operators, regulators, policymakers, and the public to transform not only the makeup of a region's generator fleet, but also the controls, regulations, and markets that dictate how this fleet is operated.

Acknowledgements

This work was supported by the Precourt Institute for Energy Efficiency, the National Science Foundation Graduate Research Fellowship, and the Stanford Graduate Fellowship. The authors would like to thank Tom Mancini and Andrew Mills for their expertise and suggestions during the model improvement stage of this work; Eric Stoutenburg, Gil Masters, and John Weyant for helpful comments during the preparation of this manuscript; and the Jacobson research group for their thoughtful insights throughout.

References

- 1 R. E. Sims, H.-H. Rogner and K. Gregory, *Energy Policy*, 2003, **31**, 1315–1326.
- 2 M. Lenzen and J. Munksgaard, *Renewable Energy*, 2002, **26**, 339–362.
- 3 D. Weisser, *Energy*, 2007, **32**, 1543–1559.
- 4 A. Stoppato, *Energy*, 2008, **33**, 224–232.
- 5 R. Crawford, *Renewable Sustainable Energy Rev.*, 2009, **13**, 2653–2660.
- 6 M. Z. Jacobson, *Energy Environ. Sci.*, 2009, **2**, 148–173.
- 7 R. Gross, P. Heptonstall, D. Anderson, T. Green, M. Leach and J. Skea, *The Costs and Impacts of Intermittency: An assessment of the evidence on the costs and impacts of intermittent generation on the British electricity network*, UK Energy Research Centre Technical Report, 2006.
- 8 B. Parsons, M. Milligan, B. Zavadil, D. Brooks, B. Kirby, K. Dragoon and J. Caldwell, *Wind Energy*, 2004, **7**, 87–108.
- 9 J. F. DeCarolis and D. W. Keith, *The Electricity Journal*, 2005, **18**, 69–77.
- 10 D. J. Swider and C. Weber, *European Transactions on Electrical Power*, 2007, **17**, 151–172.
- 11 E. Denny and M. O'Malley, *IEEE Trans. Power Syst.*, 2006, **21**, 341–347.
- 12 M. Fripp, *Environ. Sci. Technol.*, 2011, **45**, 9405–9412.
- 13 E. K. Hart and M. Z. Jacobson, *Renewable Energy*, 2011, **36**, 2278–2286.
- 14 W. Katzenstein and J. Apt, *Environ. Sci. Technol.*, 2009, **43**, 253–258.
- 15 E. K. Hart, E. D. Stoutenburg and M. Z. Jacobson, *Proc. IEEE*, 2012, **100**, 322–334.
- 16 California Energy Commission, *Large Solar Energy Projects*, <http://www.energy.ca.gov/siting/solar/index.html>, 2009.
- 17 Bureau of Land Management, *Solar Energy Study Areas*, http://www.blm.gov/wo/st/en/prog/energy/solar_energy/Solar_Energy_Study_Areas.html, 2009.
- 18 L. Frantzis, S. Graham and J. Paidipati, *California rooftop photovoltaic (PV) resource assessment and growth potential by county*, Navigant Consulting, California Energy Commission PIER Final Project Report CEC-500-2007-048, 2007.
- 19 E. Sison-Lebrilla and V. Tiangco, *Geothermal strategic value analysis*, California Energy Commission Staff Paper CEC-500-2005-105-SD, 2005.
- 20 3TIER, *Development of Regional Wind Resource and Wind Plant Output Datasets*, SR-550–47676, 2010.
- 21 O. Ekren and B. Y. Ekren, *Appl. Energy*, 2010, **87**, 592–598.
- 22 W. Zhou, C. Lou, Z. Li, L. Lu and H. Yang, *Appl. Energy*, 2010, **87**, 380–389.
- 23 F. Fusco, G. Nolan and J. V. Ringwood, *Energy*, 2010, **35**, 314–325.
- 24 H. Lund, *Renewable Energy*, 2006, **31**, 503–515.
- 25 C. Kavalec and T. Gorin, *California Energy Demand 2010–2020, Adopted Forecast*, California Energy Commission Commission Report CEC-200-2009-012-CMF, 2009.